

## Photoacoustic generation for a spherical absorber with impedance mismatch with the surrounding media

J. M. Sun and Bernard S. Gerstman

*Physics Department, Florida International University, University Park, Miami, Florida 33199*

(Received 13 July 1998)

Pressure generation in a spherical absorber due to energy deposition from pulsed lasers is studied. For a variety of conditions, analytical solutions are derived that allow quick computation of exact results. For the special case of identical acoustic impedance, the pressure transient spreads to the surrounding medium by a single compressive pulse followed by a tensile pulse at the end of illumination. For the general case of impedance mismatch, the pressure transient is in the form of a series of dampened compressive and tensile pressure pulses. In this paper both the amplitude ratio and the sign of consecutive pressure pulses are determined analytically, and are shown to be dependent upon the impedance mismatch. For laser pulses of duration much less than the absorber's characteristic oscillation time, a stress confinement limit is reached for most of the absorber, but a sharp tensile stress in the core region of the sphere is predicted. This region of high stress is defined by  $r \leq r_c$ , and we show that  $r_c$  is proportional to the laser pulse duration  $\tau_0$ . Upon further shortening of the laser pulse duration, the strength of this tensile stress continues to increase while its spatial distribution is sharpened. This observation has relevance to a number of experiments where laser-induced pressure transients cause the absorber to fracture. [S1063-651X(99)08605-5]

PACS number(s): 42.62.Be, 43.20.+g

### I. INTRODUCTION

With the widespread use of lasers in medical and commercial applications, a physical understanding of the interaction between the laser pulse and absorbing material is both desirable and necessary. These investigations have significant interest in terms of the basic physics involved in the nonlinear interplay of optical and acoustic phenomena [1]. They are also of interest from a practical point of view. Light can affect material through diverse physical means which include thermal [2–4], electrical [5,6], and chemical [7] processes. Even within the category of thermal effects, processes involving thermomechanical effects can follow very different underlying physics from the purely thermal-heating-conduction process [3]. In this paper, our interest focuses on one particular thermomechanical effect, which involves temperature rise, pressure buildup, and mechanical expansion. Processes like this are referred to as thermoelastic, in distinction from another thermomechanical process—the optical breakdown which involves evaporation, generation of hot plasmas upon energy absorption, and mechanical expansion [8].

The theoretical investigation of thermoelastic effects began with the two Danilovskaya problems (1950–1952) [9]. The first Danilovskaya problem is a half-space model with an abrupt change of temperature on the surface and no conduction between media. The second problem solves the same model with heat conductance taken into account. In either case a pressure transient results due to the abrupt temperature change. Generalizations of the model to other geometries and temperature distributions have been made [10–13]. In particular, Hu developed expressions for calculating the pressure outside the absorbing region for a spherical absorber [14]. Most of these analytical results, however, are obtained under the special condition that the absorbing region and the

surrounding medium are parts of one homogeneous material and hence have identical acoustic impedances.

There has been renewed interest in thermoelastic effects due to the increasing use of shorter laser pulses in biological systems. The generation of high pressure is desired in some cases such as cold ablation, while in other cases it is the cause of unwanted damage [15]. Because of the heterogeneous nature of, and uneven absorption in, most biosystems, an accurate prediction of pressure transients cannot be achieved without taking into account the difference in acoustic properties between different parts of the system. A formulation with general applicability is needed.

In this paper, we have studied laser interactions with a single spherical uniform absorber surrounded by a transparent medium. With the assumption of linear mechanical responses by the absorber and medium, an analytic solution for pressure transients is obtained. Heat conduction is not included when the pulse duration  $\tau_0$  is much shorter than characteristic heat conduction times. Nonlinearity in propagation [16], or the possibility of phase changes such as bubble formation [17] are not considered within the analytical framework. The value of the analytic solution is however, twofold: (1) It gives an explicit relation between the laser input parameters, the mechanical properties of the system, and the generated pressure transients. (2) Even for systems with significant nonlinearity, the solutions provide a detailed description of photoacoustic generation at times before the nonlinearities are manifested, and allow a prediction of nonlinear events, such as a compressive portion of the transient which would eventually develop into a shock wave, or a tensile stress which might form a cold bubble inside the liquid. Even when the nonlinear events occur, there is always a range of influence outside which the linear solutions are still approximately valid [16]. For example, formation of a shock wave far away from the absorber will not affect the pressure changes at the absorber until after enough time has elapsed

for the effect of the shock disturbance to travel back to the absorber.

Our analytic solution exhibits the following interesting features for the pressure transient: For identical impedances of the absorber and the medium, the pressure transient spreads to the medium in a compressive pulse, which is followed by a tensile pulse. For the general case of impedance mismatch, the pressure transient is in the form of a series of pulses of decreasing amplitudes. The damping rate, or amplitude ratio between successive pressure peaks, depends on the mismatch; the more similar the mechanical properties, the faster the pulses decay. For identical densities but different bulk moduli, the pulses spreading out to the medium are exactly parabolic in shape. If the absorber has a larger modulus than the surrounding medium, the consecutive pulses have the same sign; that is, a series of compressive pulses occur during the illumination, followed by a series of tensile pulses after the illumination. If the opposite is true, so that the medium has a higher bulk modulus, the consecutive pulses have opposite signs; that is, compressive and tensile pulses alternate with each other. For the general case of different densities, the mathematical form of the pressure is more complicated. However, the above mentioned features remain for moderate density mismatch.

Another interesting feature of this model is the prediction of a sharp tensile stress in the core of the sphere for laser pulses much shorter than the oscillation time of the absorber. Pulses of this length are expected to be in the stress confinement regime, in which the pressure amplitudes generated should become independent of pulse length. We find this not to be true in the core region. Fractures near the center of the absorber caused by tensile stress resulting from ultrashort laser pulses have been suggested by both numerical calculation [18] and experimental observation [19]. In particular, a microscopic simulation of an absorber by Zhigilei and Garrison showed the fracture effect at the center for ultrashort pulses [20]. The phenomenon, however, is still poorly understood in terms of its relation to the laser-pulse duration and its apparent violation of the stress confinement notion, and there is a lack of a quantitative basis for its prediction. An analytic model with explicit dependencies on the parameters is very helpful in understanding the various aspects of the phenomenon. Our analytic results show that the sharp tensile stress develops in the core region of the sphere at a delayed time after the short laser pulse. The delay time is equal to the time for a wave to travel from the surface of the absorber back into the center. The region is defined by  $r \leq r_c$  where  $r_c$  is a critical radius that separates inner and outer regions within the absorber that have different  $r$  dependencies for the tensile stress.  $r_c$  is proportional to the laser pulse duration  $\tau_0$ . Upon further shortening of the laser pulse duration beyond this stress confinement limit, the strength of this tensile stress continues to increase while its spatial distribution is sharpened. This is in obvious conflict with the general notion of stress confinement. Our result predicting that pressures will continue to strengthen as the pulse duration is shortened will lead to a more careful estimate of the threshold fluence for mechanical damage for ultrashort laser pulses.

A description of the model we use, as well as an outline of the steps leading to the analytic solution will be described

in Sec. II. In Sec. III we discuss our results and the implications for some real systems.

## II. MODEL AND ANALYTIC SOLUTION

Our model consists of an uniform spherical absorber surrounded by a transparent medium. The rate of energy input per unit mass  $\dot{I}_e$  is given by [2]

$$\dot{I}_e = \frac{3I_0}{4a\tau_0\rho_0} \left[ 1 - \frac{1}{2\alpha_L^2 a^2} [1 - e^{-2\alpha_L a} (1 + 2\alpha_L a)] \right], \quad (1)$$

where  $I_0$  is the incident fluence in J/cm<sup>2</sup>,  $a$  is the radius of the sphere,  $\tau_0$  is the laser pulse duration,  $\rho_0$  is the static density of the sphere, and  $\alpha_L$  is the absorption coefficient.

To be consistent with notation, we use  $r$  (a Lagrangian) to denote the initial position of an element of mass, and  $\mathbf{u}(r, t)$  (a Eulerian) its corresponding position vector at time  $t$ . In this notation, an element of mass at  $\mathbf{u}(r, t)$  starts at  $r$ , i.e.,  $\mathbf{u}(r, t=0) = \mathbf{r}$ . The mathematical dot operation  $\dot{f}(t)$  means a total time derivative for a fixed mass. The spatial derivative  $\nabla$  is taken with respect to  $r$  while the spatial derivative with respect to the Eulerian coordinate is explicitly denoted as  $\nabla_u$ . With this notation, the equation of motion for a point inside the sphere is

$$\rho \ddot{\mathbf{u}} = -\nabla_u P, \quad (2)$$

where  $P$  is the pressure, and  $\rho$  is the time varying density which is related to the static density by mass conservation. For spherical geometry,

$$\rho_0 r^2 = u^2 \rho \frac{\partial u}{\partial r}, \quad (3)$$

where  $u$  is the radial (only) component of  $\mathbf{u}$ . With Eq. (3), the equation of motion now reads

$$\rho_0 r^2 \ddot{\mathbf{u}} = -u^2 \nabla P. \quad (4)$$

In this paper, we use the assumption that the bulk modulus  $B$  and thermal-expansion coefficient  $\alpha$  are constant, which excludes the occurrence of nonlinear propagation. With these approximations of constant mechanical parameters, the equation of state can be written as

$$\frac{\dot{v}}{v} = -\frac{\dot{P}}{B} + \alpha \dot{T}, \quad (5)$$

where  $v = 1/\rho$  is the specific volume and is related to  $\mathbf{u}$  by the continuity equation ( $\dot{v} = \partial v / \partial t + \dot{\mathbf{u}} \cdot \nabla_u v$ ), which allows us to write Eq. (5) as

$$\frac{\dot{v}}{v} = \nabla_u \cdot \dot{\mathbf{u}} = -\frac{\dot{P}}{B} + \alpha \dot{T}. \quad (6)$$

Energy conservation in a unit volume takes the form

$$\rho \dot{I}_e - \nabla_u \cdot (P \dot{\mathbf{u}}) = \rho (\dot{e}_i + \dot{e}_k), \quad (7)$$

where  $\dot{e}_i = T \dot{s} - P \dot{v}$  is the internal energy rate of change per unit mass, and  $\dot{e}_k = \dot{\mathbf{u}}^2 / 2$  is the kinetic energy per unit mass.  $s$  is the specific entropy.

Use of Eqs. (2) and (6) in Eq. (7) shows that, at any instant, the absorbed laser energy can be expressed as the product of the temperature and the change of entropy of the absorber. This energy is used to raise the temperature of the absorber and change its volume,

$$\dot{I}_e = T\dot{s} = c_v \dot{T} + B\alpha T\dot{v}, \quad (8)$$

where  $c_v$  is the specific heat.

The equation of motion [Eq. (4)], the equation of state [Eq. (6)], and the conservation of energy [Eq. (8)] constitute the governing equations for the absorber. Similar equations can be obtained for the medium. The equation of motion is

$$\rho_{m0} r^2 \ddot{\mathbf{u}} = -u^2 \nabla P. \quad (9)$$

The equation of state is

$$\nabla_{\mathbf{u}} \cdot \dot{\mathbf{u}} = -\frac{\dot{P}}{B_m}, \quad (10)$$

where the subscript  $m$  is for the medium. Equation (10) has no temperature term because we are looking at times much shorter than the heat conduction time into the medium. Since heat conduction is excluded,  $B_m$  is the adiabatic bulk modulus. The set of equations (4), (6), (8), (9), and (10) can be solved by numerical means subject to the following boundary conditions: (1)  $\delta \mathbf{u}$  is strictly zero at  $r=0$  and  $\infty$ , (2)  $\dot{\mathbf{u}}$  is zero at  $t=0$ , and (3)  $\mathbf{u}$  and  $P$  are continuous at  $r=a$ .

Even with the assumption of constant mechanical parameters, the set of equations is still nonlinear due to the spherical geometry and the coupling between volume expansion and heating in Eq. (8). However, unlike the nonlinearity associated with a high and variable compressibility for a gas or liquid, this nonlinearity has little effect on most systems and conditions of interest. We can assume that  $\delta u = u - r \ll r$  and its corresponding effect on heating is negligible. Dropping the second term on the right of Eq. (8), we have

$$\delta T = T - T(0) = f(r) \gamma(t),$$

$$\gamma(t) = \frac{\dot{I}_e}{c_v} [t\theta(t) - (t - \tau_0)\theta(t - \tau_0)], \quad (11)$$

where  $f(r)$  is the spatial distribution of the energy deposition  $\dot{I}_e$ , and  $\gamma(t)$  is its time dependence. We can then expand the set of Eqs. (4), (6), (8), (9), and (10) to first order in  $\delta \mathbf{u}$  and  $\delta T$ . The resulting equations are the following. For  $r \leq a$ ,

$$\rho_0 \delta \ddot{\mathbf{u}} = B \nabla [\nabla \cdot \delta \mathbf{u}] - \alpha B \nabla \delta T,$$

$$\delta P = -B \nabla \cdot \delta \mathbf{u} + \alpha B \delta T. \quad (12a)$$

For  $r > a$ ,

$$\rho_{m0} \delta \ddot{\mathbf{u}} = B_m \nabla [\nabla \cdot \delta \mathbf{u}],$$

$$\delta P = -B_m \nabla \cdot \delta \mathbf{u}. \quad (12b)$$

Since the system has spherical symmetry,  $\mathbf{u}$  has no curl, and we can therefore write  $\delta \mathbf{u} = \nabla \phi$ . The equations now become the following. For  $r \leq a$ ,

$$\frac{1}{c^2} \ddot{\phi} = \nabla^2 \phi - \alpha \delta T,$$

$$\delta P = -\rho_0 \dot{\phi}, \quad (13a)$$

For  $r > a$ ,

$$\frac{1}{c_m^2} \ddot{\phi} = \nabla^2 \phi,$$

$$\delta P = -\rho_{m0} \dot{\phi}, \quad (13b)$$

where  $c^2 = B/\rho_0$  and  $c_m^2 = B_m/\rho_{m0}$ . The boundary conditions are now (1)  $\nabla \phi = 0$  at  $r=0$  and  $\infty$  for all  $t$ ; (2)  $\phi = 0$  and  $\dot{\phi} = 0$  for  $t=0$ ; and (3) for all  $t$ ,

$$\nabla \phi|_{r=a^-} = \nabla \phi|_{r=a^+},$$

$$\rho_0 \dot{\phi}|_{r=a^-} = \rho_{m0} \dot{\phi}|_{r=a^+}.$$

To solve Eqs. (13a) and (13b), we follow the strategy of Hu [14], which is to perform a Laplace transformation on time before applying the Green's-function method in space. The direct use of space-time Green's-function methods involves multiple integrals, and is unnecessarily more complicated mathematically.

Denoting the Laplace transform of  $\phi$  as  $\Phi(r, s) = \mathcal{L}[\phi(r, t)]$  and using the initial boundary condition at  $t=0$ , we have the following. For  $r \leq a$ ,

$$\nabla^2 \Phi - \frac{s^2}{c^2} \Phi = \alpha f(r) \gamma(s),$$

$$P(r, s) = -s^2 \rho_0 \Phi. \quad (14a)$$

For  $r > a$ ,

$$\nabla^2 \Phi - \frac{s^2}{c_m^2} \Phi = 0,$$

$$P(r, s) = -s^2 \rho_{m0} \Phi, \quad (14b)$$

where  $P(r, s)$  and  $\gamma(s)$  are the Laplace transforms of  $\delta P(r, t)$  and  $\gamma(t)$ , respectively. The boundary conditions at  $r=a$  are now

$$\nabla \Phi|_{r=a^-} = \nabla \Phi|_{r=a^+},$$

$$\rho_0 \Phi|_{r=a^-} = \rho_{m0} \Phi|_{r=a^+}.$$

The Green's function  $G(r, r')$  is defined as

$$\Phi(r, s) = \alpha \gamma(s) \int_0^a dr' f(r') G(r, r'), \quad (15)$$

where  $r' \leq a$ , since the energy deposition function  $f(r)$  is nonzero only inside the sphere.  $G(r, r')$  satisfies the following equations:

$$\nabla^2 G(r, r') - \frac{s^2}{c^2} G(r, r') = \delta(r - r'), \quad r \leq a,$$

$$\nabla^2 G(r, r') - \frac{s^2}{c_m^2} G(r, r') = \delta(r - r'), \quad r > a. \quad (16)$$

The Green's function  $G(r, r')$  is subject to the same boundary conditions as  $\Phi$ . The Green's function satisfying the boundary conditions is

$$G(r, r') = \begin{cases} g^{-1} Q(r') \frac{r' c}{sr} \sinh\left(\frac{sr}{c}\right), & r < r' < a \\ g^{-1} Q(r) \frac{r' c}{sr} \sinh\left(\frac{sr'}{c}\right), & r' < r < a \\ g^{-1} \frac{\rho_0 r' a}{\rho_{m0} r} \sinh\left(\frac{sr'}{c}\right) \exp\left(-\frac{s}{c_m}(r-a)\right), & r' < a < r, \end{cases} \quad (17)$$

where  $Q$  is given by

$$Q(x) = \frac{\rho_0}{\rho_{m0}} \left(\frac{sa}{c_m} + 1\right) \sinh\left(\frac{s}{c}(a-x)\right) + \frac{sa}{c} \cosh\left(\frac{s}{c}(a-x)\right) - \sinh\left(\frac{s}{c}(a-x)\right),$$

and  $g$  is given as the following:

$$g = \left[ 1 - \frac{\rho_0}{\rho_{m0}} \left(\frac{sa}{c_m} + 1\right) \right] \sinh\left(\frac{sa}{c}\right) - \frac{sa}{c} \cosh\left(\frac{sa}{c}\right), \quad (18a)$$

and  $g^{-1}$  is given by the following expansion:

$$g^{-1} = -2 \sum_{k=0}^{\infty} e^{-(sa/c)(1+2k)} \frac{A_2^k}{A_1^{1+k}},$$

$$A_1 = h_1 s + \Delta_\rho,$$

$$A_2 = h_2 s + \Delta_\rho, \quad (18b)$$

where we have introduced the parameters  $h_1$ ,  $h_2$ , and  $\Delta_\rho$ :

$$h_1 = (\rho_0 a) / (\rho_{m0} c_m) + a/c,$$

$$h_2 = (\rho_0 a) / (\rho_{m0} c_m) - a/c,$$

$$\Delta_\rho = \frac{\rho_0}{\rho_{m0}} - 1. \quad (19)$$

The solution for  $\Phi$  depends on the explicit choice for  $f(r)$ . For uniform absorption throughout the sphere, a step function is the obvious choice. However, direct use of a step function with a discontinuity at  $r = a$  leads to mathematical complications later. To avoid this, we let

$$f(r) = \begin{cases} 1 - \exp[-\eta(a-r)], & r \leq a \\ 0, & r > a, \end{cases} \quad (20)$$

and take  $\eta \rightarrow \infty$  later. Such a complication is unfortunately necessary. Failing to do so will lead to a discontinuity in  $u$ . With  $f(r)$  given by Eq. (20), we find the following. For  $r \leq a$ ,

---


$$P(r, s) = B \alpha \gamma(s) + B \alpha \gamma(s) \mu(s), \quad (21a)$$

$$\mu(s) = \frac{c}{4gr} \left[ (Z_0 - Z_1^- A_1 + Z_1^+ A_2) \exp\left(\frac{sr}{c}\right) + (-Z_0 + Z_1^- A_1 - Z_1^+ A_2) \exp\left(-\frac{sr}{c}\right) \right. \\ \left. + (Z_2^- - Z_2^+) A_1 \exp\left(\frac{sa}{c} - \eta(a-r)\right) + (-Z_2^- + Z_2^+) A_2 \exp\left(-\frac{sa}{c} - \eta(a-r)\right) \right. \\ \left. + (-Z_3^- + Z_3^+) A_1 \exp\left(\frac{s}{c}(a-r) - \eta a\right) + (Z_3^- - Z_3^+) A_2 \exp\left(-\frac{s}{c}(a-r) - \eta a\right) \right].$$

For  $r > a$ ,

$$P(r, s) = B \alpha \gamma(s) \mu(s),$$

$$\mu(s) = \frac{as}{2gr} \left[ \left(\frac{1}{s} - Z_1^+\right) \exp\left(-\frac{s}{c_m}(r-a) + \frac{sa}{c}\right) + \left(-\frac{1}{s} + Z_1^-\right) \exp\left(-\frac{s}{c_m}(r-a) - \frac{sa}{c}\right) \right. \\ \left. + (-Z_3^- + Z_3^+) \exp\left(-\frac{s}{c_m}(r-a) - \eta a\right) \right], \quad (21b)$$

where  $Z_0$ ,  $Z_1^\pm$ ,  $Z_2^\pm$ , and  $Z_3^\pm$  are defined as

$$Z_0 = \frac{2a}{c}, \quad Z_1^\pm = (a\eta + 1) / (s \pm c\eta) \mp (c\eta) / (s \pm c\eta)^2,$$

$$Z_2^\pm = (r\eta + 1)/(s \pm c\eta) \mp (c\eta)/(s \pm c\eta)^2, \quad Z_3^\pm = 1/(s \pm c\eta) \mp (c\eta)/(s \pm c\eta)^2. \quad (22)$$

Using the expansion of  $g^{-1}$  in Eq. (18), we can recast  $\mu(s)$  into a series:

$$\mu(s) = \frac{c}{2r} \sum_{k=0}^{\infty} B_k(r, s). \quad (23a)$$

For  $r \leq a$ ,

$$\begin{aligned} B_k(r, s) = & \frac{A_2^k}{A_1^{1+k}} \exp\left(-2k \frac{sa}{c}\right) \left[ (-Z_0 + Z_1^- A_1 - Z_1^+ A_2) \exp\left(-\frac{s}{c}(a-r)\right) \right. \\ & + (Z_0 - Z_1^- A_1 + Z_1^+ A_2) \exp\left(-\frac{s}{c}(a+r)\right) + (Z_2^+ - Z_2^-) A_1 \exp[-\eta(a-r)] \\ & + (Z_2^- - Z_2^+) A_2 \exp\left(-2a \frac{s}{c} - \eta(a-r)\right) + (Z_3^- - Z_3^+) A_1 \exp\left(-\frac{sr}{c} - \eta a\right) \\ & \left. + (-Z_3^- + Z_3^+) A_2 \exp\left(-\frac{s}{c}(2a-r) - \eta a\right) \right]. \end{aligned} \quad (23b)$$

For  $r > a$ ,

$$\begin{aligned} B_k(r, s) = & 2s \frac{a}{c} \frac{A_2^k}{A_1^{1+k}} \exp\left(-2k \frac{sa}{c}\right) \left[ \left(-\frac{1}{s} + Z_1^+\right) \exp\left(-\frac{s}{c_m}(r-a)\right) + \left(\frac{1}{s} - Z_1^-\right) \exp\left(-\frac{s}{c_m}(r-a) - \frac{2sa}{c}\right) \right. \\ & \left. + (Z_3^- - Z_3^+) \exp\left(-\frac{s}{c_m}(r-a) - \frac{sa}{c} - \eta a\right) \right]. \end{aligned} \quad (23c)$$

The linearities of the system and Laplace transform enable us to write

$$\delta P(r, t) = \theta(t) P_L(r, t) - \theta(t - \tau_0) P_L(r, t - \tau_0) \quad (24)$$

where  $P_L(r, t)$  is the pressure that would be generated if the laser illumination was continued at the same intensity indefinitely. The effect of turning off the laser is achieved by superimposing a negative signal after  $t = \tau_0$ . This fact is also obvious from Eq. (11). The  $P_L(r, t)$  is now the following.

For  $r \leq a$ ,

$$P_L(r, t) = B\alpha \frac{I_e}{c_v} \left[ t + \frac{c}{2r} \sum_{k=0}^{\infty} t * b_k(r, t) \right]. \quad (25a)$$

For  $r > a$ ,

$$P_L(r, t) = B\alpha \frac{I_e c}{2rc_v} \sum_{k=0}^{\infty} t * b_k(r, t), \quad (25b)$$

where  $b_k(r, t) = \mathcal{L}^{-1} B_k(r, s)$ , and  $f(t) * g(t) = \int_0^t dt' f(t-t')g(t')$  is the convolution of  $f$  and  $g$ .

The general solution for the pressure transient has a complicated mathematical form. In some special cases, simple and illustrative results can be obtained.

(a)  $\rho_{m0} = \rho_0$  and  $c_m = c$ . In this case, we have  $\Delta_\rho = h_2 = A_2 = 0$ , and Eq. (23) shows that all  $B_k$  are zero except  $B_0$ .  $B_0$  is simplified as follows: For  $r \leq a$ ,

$$\begin{aligned} B_0 = & \left(-\frac{1}{s} + Z_1^-\right) \exp\left(-\frac{s}{c}(a-r)\right) \\ & + \left(\frac{1}{s} - Z_1^-\right) \exp\left(-\frac{s}{c}(a+r)\right) \\ & + (-Z_2^- + Z_2^+) \exp[-\eta(a-r)] \\ & + (Z_3^- - Z_3^+) \exp\left(-\frac{s}{c}r - \eta a\right). \end{aligned} \quad (26a)$$

For  $r > a$ ,

$$\begin{aligned} B_0 = & \left(-\frac{1}{s} + Z_1^+\right) \exp\left(-\frac{s}{c}(r-a)\right) \\ & + \left(\frac{1}{s} - Z_1^-\right) \exp\left(-\frac{s}{c}(r+a)\right) \\ & + (Z_3^- - Z_3^+) \exp\left(-\frac{s}{c}r - \eta a\right). \end{aligned} \quad (26b)$$

The inverse Laplace transform of  $B_0(r, s)$ ,  $b_0(r, t)$  is given by the following, in which we drop terms which make no contribution in the limit of  $\eta \rightarrow \infty$ . For  $r \leq a$  (assuming  $r < (a-r)$ , the converse situation does not affect the final result),

$$b_0(r,t) = \begin{cases} -\eta(r+ct)\exp\left[\eta c\left(t-\frac{a-r}{c}\right)\right], & 0 < t \leq \frac{r}{c} \\ -\eta(r+ct)e^{\eta c[t-(a-r)/c]} + \eta(ct-r)e^{\eta c[t-(a+r)/c]}, & \frac{r}{c} < t \leq \frac{a-r}{c} \\ -1 + \eta(ct-r)\exp\left[\eta c\left(t-\frac{a+r}{c}\right)\right], & \frac{a-r}{c} < t \leq \frac{a+r}{c} \\ 0, & \frac{a+r}{c} < t. \end{cases} \quad (27a)$$

For  $r > a$ ,

$$b_0(r,t) = \begin{cases} 0, & 0 < t \leq \frac{r-a}{c} \\ -1 + \eta(r-ct)\exp\left[-\eta c\left(t-\frac{r-a}{c}\right)\right], & \frac{r-a}{c} < t \leq \frac{r}{c} \\ -1 + \eta(ct-r)\exp\left[\eta c\left(t-\frac{r+a}{c}\right)\right], & \frac{r}{c} < t \leq \frac{r+a}{c} \\ 0, & \frac{r+a}{c} < t. \end{cases} \quad (27b)$$

After computing the convolution  $b*t$ , we obtain simple results for the pressure transient: For  $r \leq a$ ,

$$P_L(r,t) = \begin{cases} B\alpha \frac{\dot{I}_e}{c_v} t, & 0 < t \leq \frac{a-r}{c} \\ B\alpha \frac{\dot{I}_e}{c_v} \left[ t - \frac{c}{4r} \left( t - \frac{a-r}{c} \right) \left( t + \frac{a+r}{c} \right) \right], & \frac{a-r}{c} < t \leq \frac{a+r}{c} \\ 0, & \frac{a+r}{c} < t. \end{cases} \quad (28a)$$

For  $r > a$ ,

$$P_L(r,t) = \begin{cases} 0, & 0 < t \leq \frac{r-a}{c} \\ B\alpha \frac{\dot{I}_e c}{4rc_v} \left[ \frac{a^2}{c^2} - \left( t - \frac{r}{c} \right)^2 \right], & \frac{r-a}{c} < t \leq \frac{r+a}{c} \\ 0, & \frac{r+a}{c} < t. \end{cases} \quad (28b)$$

For this special case, the pressure transient outside the sphere Eq. (28b) was previously obtained by Hu in his study of pressure generation in an aqueous medium by self-focusing and self-defocusing effects [14].

(b)  $\rho_{m0} = \rho_0$  and  $c_m \neq c$ . Under these conditions, we have  $\Delta_\rho = 0$ ,  $A_1 = h_1 s$ , and  $A_2 = h_2 s$ . All  $B_k$  are now nonzero: For  $r \leq a$ ,

$$\begin{aligned} B_k(r,s) = & \left( \frac{h_2}{h_1} \right)^k \exp\left(-2k \frac{sa}{c}\right) \left[ \left( -\frac{Z_0}{h_1 s} + Z_1^- - \frac{h_2}{h_1} Z_1^+ \right) \exp\left(-\frac{s}{c}(a-r)\right) + \left( \frac{Z_0}{h_1 s} - Z_1^- + \frac{h_2}{h_1} Z_1^+ \right) \exp\left(-\frac{s}{c}(a+r)\right) \right] \\ & + (-Z_2^- + Z_2^+) \exp[-\eta(a-r)] + (Z_2^- - Z_2^+) \frac{h_2}{h_1} \exp\left(-2a \frac{s}{c} - \eta(a-r)\right) + (Z_3^- - Z_3^+) \exp\left(-\frac{sr}{c} - \eta a\right) \\ & + (-Z_3^- + Z_3^+) \frac{h_2}{h_1} \exp\left(-\frac{s}{c}(2a-r) - \eta a\right). \end{aligned} \quad (29a)$$

For  $r > a$ ,

$$B_k(r,s) = \frac{2a}{h_1 c} \left(\frac{h_2}{h_1}\right)^k \exp\left(-2k \frac{sa}{c}\right) \left[ \left(-\frac{1}{s} + Z_1^+\right) \exp\left(-\frac{s}{c_m}(r-a)\right) + \left(\frac{1}{s} - Z_1^-\right) \exp\left(-\frac{s}{c_m}(r-a) - \frac{2sa}{c}\right) \right. \\ \left. + (Z_3^- - Z_3^+) \exp\left(-\frac{s}{c_m}(r-a) - \frac{sa}{c} - \eta a\right) \right]. \tag{29b}$$

The inverse Laplace transform of  $B_k(r,s)$ ,  $b_k(r,t)$  is given by the following (we again drop terms which make no contribution in the limit of  $\eta \rightarrow \infty$ ): For  $r \leq a$ , we define a time parameter that is relevant for each value of  $k$ ,  $t_k = t - 2k(a/c)$ :

$$b_k(r,t) = \left(\frac{h_2}{h_1}\right)^k \begin{cases} \left\{ -\eta(r+ct_k) \exp\left[ c \eta \left( t_k - \frac{a-r}{c} \right) \right] \right\}, & 0 < t_k \leq \frac{r}{c} \\ \left\{ \eta \left[ -(r+ct_k) \exp\left[ c \eta \left( t_k - \frac{a-r}{c} \right) \right] + (ct_k-r) \exp\left[ c \eta \left( t_k - \frac{a+r}{c} \right) \right] \right\}, & \frac{r}{c} < t_k \leq \frac{a-r}{c} \\ \left\{ -\frac{2a}{ch_1} + \frac{h_2}{h_1} \eta(r+ct_k-2a) \exp\left[ -c \eta \left( t_k - \frac{a-r}{c} \right) \right] + \eta(ct_k-r) \exp\left[ c \eta \left( t_k - \frac{a+r}{c} \right) \right] \right\}, & \frac{a-r}{c} < t_k \leq \frac{a+r}{c} \\ \left\{ \eta \frac{h_2}{h_1} \left[ (r+ct_k-2a) \exp\left[ -c \eta \left( t_k - \frac{a-r}{c} \right) \right] + (r-ct_k+2a) \exp\left[ c \eta \left( t_k - \frac{a+r}{c} \right) \right] \right\}, & \frac{a+r}{c} < t_k \leq \frac{2a-r}{c} \\ \left\{ \eta \frac{h_2}{h_1} \left[ (2a-r-ct_k) \exp\left[ c \eta \left( t_k - \frac{3a-r}{c} \right) \right] + (r-ct_k+2a) \exp\left[ c \eta \left( t_k - \frac{a+r}{c} \right) \right] \right\}, & \frac{2a-r}{c} < t_k \leq \frac{2a}{c} \\ 0, & \frac{2a}{c} < t_k. \end{cases} \tag{30a}$$

For  $r > a$ , the important time parameter is defined as  $t_k = t - 2k(a/c) - [(r-a)/c_m]$ ,

$$b_k(r,t) = \frac{2a}{ch_1} \left(\frac{h_2}{h_1}\right)^k \begin{cases} 0, & t_k \leq 0 \\ \left[ -1 + \eta(a-ct_k) \exp(-c \eta t_k) \right], & 0 \leq t_k \leq \frac{a}{c} \\ \left\{ -1 + \eta(ct_k-a) \exp\left[ c \eta \left( t_k - \frac{2a}{c} \right) \right] \right\}, & \frac{a}{c} < t_k \leq \frac{2a}{c} \\ 0, & \frac{2a}{c} < t_k. \end{cases} \tag{30b}$$

The pressure transients are given by Eqs. (25a) and (25b), and the following convolutions  $b^*t$ : For  $r \leq a$ ,

$$\frac{c}{2r} t^* b_k = -\frac{a}{h_1} \left(\frac{h_2}{h_1}\right)^k \begin{cases} 0, & 0 < t_k \leq \frac{a-r}{c} \\ \frac{1}{2r} \left( t_k - \frac{a-r}{c} \right) \left( t_k + h_1 + h_2 - \frac{a-r}{c} \right), & \frac{a-r}{c} < t_k \leq \frac{a+r}{c} \\ \frac{2}{c} (t_k + h_2), & \frac{a+r}{c} < t_k. \end{cases} \tag{31a}$$

For  $r > a$ ,

$$\frac{c}{2r} t^* b_k = \begin{cases} 0, & t_k \leq 0 \\ \frac{a}{2rh_1} \left(\frac{h_2}{h_1}\right)^k t_k \left( \frac{2a}{c} - t_k \right), & 0 < t_k \leq \frac{2a}{c} \\ 0, & \frac{2a}{c} < t_k. \end{cases} \tag{31b}$$

(c) Finally,  $\rho_{m0} \neq \rho_0$  and  $c_m \neq c$ . For this most general case, the mathematical form is complicated. The inverse Laplace transform of  $B_k(r,s)$ ,  $b_k(r,t)$  is given by the following (again dropping terms which make no contribution in the limit of  $\eta \rightarrow \infty$ ): For  $r \leq a$ , define  $t_k = t - 2k(a/c)$ :

$$b_k(r,t) = \begin{cases} \left( \frac{h_2}{h_1} \right)^k \left\{ -\eta(r+ct_k) \exp \left[ c \eta \left( t_k - \frac{a-r}{c} \right) \right] \right\}, & 0 < t_k \leq \frac{r}{c} \\ \left( \frac{h_2}{h_1} \right)^k \left\{ \eta \left[ -(r+ct_k) \exp \left[ c \eta \left( t_k - \frac{a-r}{c} \right) \right] + (ct_k-r) \exp \left[ c \eta \left( t_k - \frac{a+r}{c} \right) \right] \right\}, & \frac{r}{c} < t_k \leq \frac{a-r}{c} \\ \left( \frac{h_2}{h_1} \right)^k \left\{ \frac{h_2}{h_1} (r+ct_k-2a) \exp \left[ -c \eta \left( t_k - \frac{a-r}{c} \right) \right] + (ct_k-r) \exp \left[ c \eta \left( t_k - \frac{a+r}{c} \right) \right] \right\} - \zeta_{s_0}^k \left( t_k - \frac{a-r}{c} \right), & \frac{a-r}{c} < t_k \leq \frac{a+r}{c} \\ \left( \frac{h_2}{h_1} \right)^{k+1} \left\{ \eta \left[ (r+ct_k-2a) \exp \left[ -c \eta \left( t_k - \frac{a-r}{c} \right) \right] + (r-ct_k+2a) \exp \left[ c \eta \left( t_k - \frac{a+r}{c} \right) \right] \right\} + \zeta_{s_0}^k \left( t_k - \frac{a+r}{c} \right) - \zeta_{s_0}^k \left( t_k - \frac{a-r}{c} \right), & \frac{a+r}{c} < t_k \leq \frac{2a-r}{c} \\ \left( \frac{h_2}{h_1} \right)^{k+1} \left\{ \eta \left[ (2a-r-ct_k) \exp \left[ c \eta \left( t_k - \frac{3a-r}{c} \right) \right] + (r-ct_k+2a) \exp \left[ c \eta \left( t_k - \frac{a+r}{c} \right) \right] \right\} + \zeta_{s_0}^k \left( t_k - \frac{a+r}{c} \right) - \zeta_{s_0}^k \left( t_k - \frac{a-r}{c} \right), & \frac{2a-r}{c} < t_k \leq \frac{2a}{c} \\ \zeta_{s_0}^k \left( t_k - \frac{a+r}{c} \right) - \zeta_{s_0}^k \left( t_k - \frac{a-r}{c} \right), & \frac{2a}{c} < t_k. \end{cases} \quad (32a)$$

For  $r > a$ , define  $t_k = t - 2k(a/c) - [(r-a)/c_m]$ :

$$b_k(r,t) = \begin{cases} 0, & t_k \leq 0 \\ \frac{2a}{ch_1} \left( \frac{h_2}{h_1} \right)^k \eta(a-ct_k) \exp(-c \eta t_k) + \Xi_{s_0}^{k-}(t_k), & 0 < t_k \leq \frac{a}{c} \\ \frac{2a}{ch_1} \left( \frac{h_2}{h_1} \right)^k \eta(ct_k-a) \exp \left[ c \eta \left( t_k - \frac{2a}{c} \right) \right] + \Xi_{s_0}^{k-}(t_k), & \frac{a}{c} < t_k \leq \frac{2a}{c} \\ \Xi_{s_0}^{k+} \left( t_k - \frac{2a}{c} \right) + \Xi_{s_0}^{k-}(t_k), & \frac{2a}{c} < t_k, \end{cases} \quad (32b)$$

where  $s_0 = -\Delta_\rho/h_1$  and  $\zeta_s^k(t)$ ,  $\Xi_s^{k\pm}(t)$  are defined as

$$\zeta_s^k(t) = \frac{a}{ck!h_1^{1+k}} \frac{\partial^k}{\partial s^k} [e^{st}(h_2s+\Delta_\rho)^k(2+h_1s+h_2s+2\Delta_\rho)], \quad \Xi_s^{k\pm}(t) = \frac{2a}{ck!h_1^{1+k}} \frac{\partial^k}{\partial s^k} \left[ e^{st}(h_2s+\Delta_\rho)^k \left( \frac{sa}{c} \pm 1 \right) \right].$$

The pressure transients are given by Eqs. (25a) and (25b), and the following convolutions  $b^*t$ : For  $r \leq a$ ,

$$\frac{c}{2r} t^* b_k = \frac{a}{2rh_1^{k+1}} \begin{cases} 0, & 0 < t_k \leq \frac{a-r}{c} \\ \left\{ \left( 2(1+\Delta_\rho) \left( t_k - \frac{a-r}{c} \right) + h_1 + h_2 \right) D_k^1(s_0,0) + 2(1+\Delta_\rho) \left[ D_k^2(s_0,0) - D_k^2 \left( s_0, t_k - \frac{a-r}{c} \right) \right] - (h_1+h_2) D_k^1 \left( s_0, t_k - \frac{a-r}{c} \right) \right\}, & \frac{a-r}{c} < t_k \leq \frac{a+r}{c} \\ \left\{ 2(1+\Delta_\rho) \left[ \frac{2r}{c} D_k^1(s_0,0) + D_k^2 \left( s_0, t_k - \frac{a+r}{c} \right) - D_k^2 \left( s_0, t_k - \frac{a-r}{c} \right) \right] + (h_1+h_2) \left[ D_k^1 \left( s_0, t_k - \frac{a+r}{c} \right) - D_k^1 \left( s_0, t_k - \frac{a-r}{c} \right) \right] \right\}, & \frac{a+r}{c} < t_k. \end{cases} \quad (33a)$$

For  $r > a$ ,

$$\frac{c}{2r} t^* b_k = \frac{a}{r h_1^{k+1}} \begin{cases} 0, & t_k \leq 0 \\ \left[ \left( t_k - \frac{a}{c} \right) D_k^1(s_0, 0) + D_k^2(s_0, 0) + \frac{a}{c} D_k^1(s_0, t_k) - D_k^2(s_0, t_k) \right], & 0 < t_k \leq \frac{2a}{c} \\ \left\{ \frac{a}{c} \left[ D_k^1(s_0, t_k) + D_k^1 \left( s_0, t_k - \frac{2a}{c} \right) \right] - D_k^2(s_0, t_k) + D_k^2 \left( s_0, t_k - \frac{2a}{c} \right) \right\}, & \frac{2a}{c} < t_k, \end{cases} \quad (33b)$$

where  $D_k^1(s, t)$  and  $D_k^2(s, t)$  have the following definitions:

$$D_k^1(s, t) = \frac{1}{k!} \frac{\partial^k}{\partial s^k} \left[ \frac{(h_2 s + \Delta_\rho)^k e^{st}}{s} \right], \quad (34a)$$

$$D_k^2(s, t) = \frac{1}{k!} \frac{\partial^k}{\partial s^k} \left[ \frac{(h_2 s + \Delta_\rho)^k e^{st}}{s^2} \right]. \quad (34b)$$

Applying the Leibnitz differential rule, we find

$$D_k^1(s, 0) = (-1)^k \frac{\Delta_\rho^k}{s^{k+1}}, \quad (35a)$$

$$D_k^2(s, 0) = (-1)^k \frac{\Delta_\rho^{k-1}}{s^{k+2}} [k s h_2 + (k+1) \Delta_\rho], \quad (35b)$$

$$D_k^{1,2}(s, t) = \sum_{i=0}^k \frac{k!}{i!(k-i)!} h_2^i (h_2 s + \Delta_\rho)^{k-i} e^{st} R_{k-i}^{1,2}(s, t), \quad (35c)$$

$$R_l^1(s, t) = \sum_{j=0}^l (-1)^j \frac{l!}{(l-j)!} \frac{t^{l-j}}{s^{j+1}}, \quad (35d)$$

$$R_l^2(s, t) = \sum_{j=0}^l (-1)^j (j+1) \frac{l!}{(l-j)!} \frac{t^{l-j}}{s^{j+2}}. \quad (35e)$$

This completes our analytic solution.

### III. RESULTS AND DISCUSSION

The various profiles of positive compressive pressure buildup and negative tensile pressure are fundamentally due to only a few physical effects. When the laser is turned on, a uniform compressive pressure increase occurs throughout the absorber, and at the same time a tensile wave due to the expansion of the absorber starts to travel in from the surface. When the pulse is turned off, the uniform compressive buildup stops, but a compressive wave traveling in from the surface commences.

In addition, reflections from the origin occur, first for the

tensile wave, and then at a time  $\tau_0$  later for the compressive wave. These reflections send waves of the opposite sign outward. The inward moving waves from the surface and their reflections superimpose their effects. Furthermore, when the mechanical impedance of the surrounding medium is not matched to the absorber, the outward moving waves are partially reflected back into the absorber, and partially transmitted. The net effect of these different pressure transients depends on their order of occurrence, which is determined by the length of the laser pulse and the point of observation. In this section, we analyze the pressure profiles for a variety of cases in which we vary the laser pulse duration compared to the relaxation time of the medium.

The general form [conditions (b) and (c)] of the pressure transient is of a series of decaying pulses. The time scale of an individual peak  $\tau_c$  is the propagation time of a sound wave from the surface of the absorber to the center and back to the surface. Equation (24) shows that the effect of turning off the laser pulse is equivalent to adding a negative signal at  $t = \tau_0$ . If  $\tau_0 \gg \tau_c$ , the positive and negative pressure transients are well separated. On the other hand, for ultrashort laser pulses  $\tau_0 \ll \tau_c$ , the overlap of the positive and negative pressure signals can lead to interesting effects such as tensile fracture inside the absorber, which we discuss later.

#### A. Long laser pulse

In this case, the positive and negative pressure pulses are well separated. The pressure amplitude is proportional to the intensity of the laser (inversely proportional to the laser pulse duration for a fixed fluence), and outside the absorber the pressure decays with a  $1/r$  factor due to the spherical geometry. During the illumination, the uniform pressure buildup inside the absorber drives a compressive pressure wave out into the medium, and a tensile wave in toward the absorber's center. At a point  $r$  inside the absorber, the pressure increases uniformly with time until this tensile wave reaches the location, at time  $t = (a-r)/c$ . The tensile disturbance relieves the pressure. The tensile wave is reflected at the spherical origin and the reflected wave, with a sign change that makes it compressive, reaches the point  $r$  at  $t = (a+r)/c$ . At  $t = 2a/c$ , the wave reflected from the origin reaches the surface and is partially transmitted out into the medium and partially reflected at the surface. This finishes one cycle of the pressure pulse. If the absorber and medium are not perfectly matched in  $B$  and  $\rho$ , the part of the wave that is reflected back from the surface will generate another round of propagation in from the surface to the origin and back to the surface. The cycle will continue with decaying amplitudes.

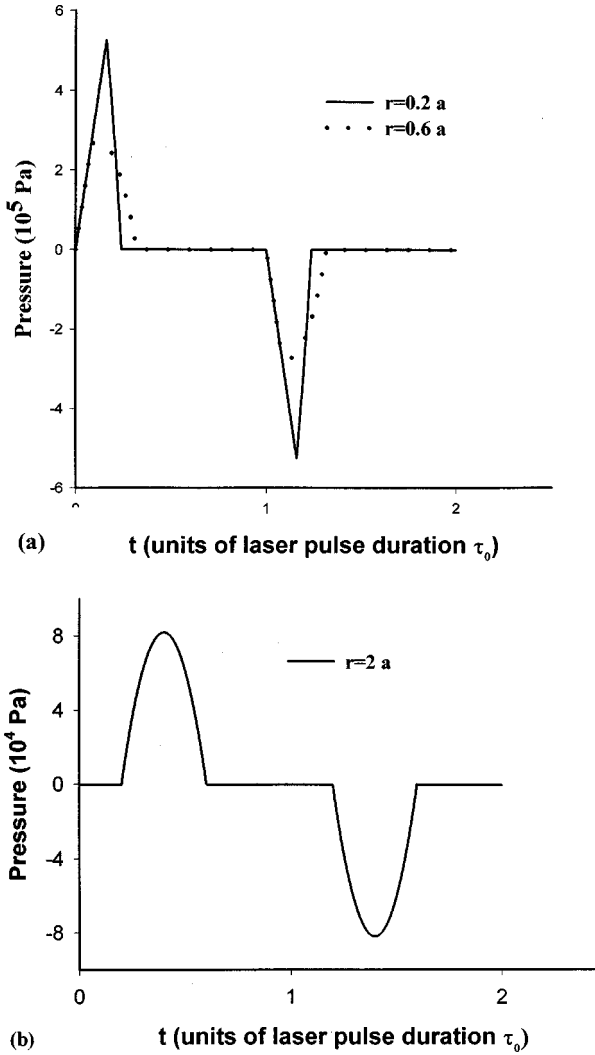


FIG. 1. Finite focusing effect in water. Gauge pressure (in pascals) vs time (in units of  $\tau_0$ , the laser pulse duration) for points inside the focus [(a)  $r=0.2a, 0.6a$ ] and outside the focus [(b)  $r=2a$ ]. The values used for water are  $\rho_0=1 \text{ g/cm}^3$ ,  $c_v=4.18 \text{ J/(g K)}$ ,  $B=2.25 \text{ GPa}$ , and  $\alpha=6.9 \times 10^{-5} \text{ K}^{-1}$ . For the laser, we use  $\tau_0=10^{-7} \text{ s}$ ,  $a=30 \mu\text{m}$ , and a deposition rate of  $\dot{I}_e=8.84 \times 10^8 \text{ J/(g s)}$ . A single pressure pulse is observed because of the perfect acoustic match at surface boundary which precludes surface reflections.

At the end of the laser pulse  $t=\tau_0$ , the “onset” of the negative laser signal sets in, and a series of pressure pulses similar to those generated during the positive laser signal will develop. However, there is a difference in that the compressive and tensile attributes will be reversed.

### 1. $\rho_{m0}=\rho_0$ and $c_m=c$

For this simplest of cases, the pressure transients inside and outside the absorber are given by Eqs. (24) and Eq. (28). There is only a single positive and a single negative pressure pulse for this case, since no reflection will occur at the mechanically perfectly matched surface boundary. A typical profile of the transients for the finite focusing effect in water is given in Fig. 1. For water, we have  $\rho_0=1 \text{ g/cm}^3$ ,  $c_v=4.18 \text{ J/(g K)}$ ,  $B=2.25 \text{ GPa}$ , and  $\alpha=6.9 \times 10^{-5} \text{ K}^{-1}$ . We choose a laser pulse of duration  $\tau_0=10^{-7} \text{ s}$  and focal size

$a=30 \mu\text{m}$ . Then  $\tau_c=2a/c=4 \times 10^{-8} \text{ s}$ , which is about half of  $\tau_0$ . The laser pulse carries an energy of  $10^{-5} \text{ J}$ , so that the resulting  $\dot{I}_e=8.84 \times 10^8 \text{ J/(g s)}$ . The resulting pressure transients as a function of time are plotted for points inside the focus, equivalent to the absorbing region in our treatment [Fig. 1(a):  $r=0.2a, 0.6a$ ] and outside the focus [Fig. 1(b):  $r=2a$ ].

For a point inside the focal sphere, the pressure increases linearly with time according to Eq. (28a) until the relieving tensile wave reaches it at  $t=(a-r)/c$ . The tensile wave comes as a result of surface expansion due to the initial internal pressure buildup. The pressure then drops parabolically according to Eq. (28a). The tensile wave continues inward, and is reflected at the spherical origin. The reflected wave undergoes an amplitude inversion and is now compressive, but is not attenuated by the reflection at the origin. The reflected compressive wave moves outward and reaches a point  $r$  at  $t=(a+r)/c$  and causes cancellation of all pressure disturbances. The pressure stays at zero after  $t=(a+r)/c$ . From Fig. 1(a) and Eq. (28a), we see that the further the point is inside, the sharper the pressure drop to zero.

For a point outside the sphere,  $r>a$ , the pressure stays at zero until the compressive pressure transient, originating from the surface, arrives at  $t=(r-a)/c$ . The pressure then increases and decreases parabolically according to Eq. (28b) [see Fig. 1(b)]. At  $t=(a+r)/c$ , the reflected wave from the origin arrives and cancels the pressure disturbance. The pressure stays at zero after  $t=(a+r)/c$  until the laser is turned off.

At  $t=\tau_0$ , the onset of the negative laser signal begins as shown in Fig. 1. The compressive aspect of the pressure transient has been changed into tensile.

### 2. $\rho_{m0}=\rho_0$ and $c_m \neq c$

For this case, because of the sound speed mismatch at the boundary, the reflected tensile wave from the origin will suffer another reflection at the surface boundary at  $t=2a/c$ . This surface reflection generates another round of propagation and reflection at the origin and a series of pressure pulses result. A strict definition of a pressure pulse for this case can be made as follows. From Eq. (31), we define the  $k$ th pulse for a point  $r$  outside the absorber as the pressure transient for times between  $2k(a/c) + [(r-a)/c_m] \leq t < 2(k+1)(a/c) + [(r-a)/c_m]$ ,  $k=0,1,2, \dots$ . The  $k$ th pulse, originating from the surface boundary at  $r=a$ , starts at  $t=2k(a/c)$  and lasts for an interval of  $2a/c$ . It propagates from the surface both outward and inward, but with different sound speeds.

We note from Eq. (31) that each pulse is exactly parabolic as a function of time outside the absorber while inside the absorber, the pulse is comprised of a parabolic portion between  $t=2k(a/c) + [(a-r)/c]$  and  $t=2k(a/c) + [(a+r)/c]$  and two linear portions outside the parabolic portion. At points outside the absorber, the partial transmittance at the boundary causes consecutive pulses to decrease in magnitude with a ratio

$$\frac{h_2}{h_1} = \frac{c-c_m}{c+c_m}. \quad (36)$$

From Eq. (36), we see that consecutive pulses have the same sign if  $c$  is greater than  $c_m$ . Since we are examining the case for  $\rho_{m0} = \rho_0$ , that means the absorber has a larger bulk modulus than the surrounding medium. If the opposite is true, consecutive pulses have opposite sign from each other. In the latter case, the pressure transient spreading to the medium has compressive and tensile pulses alternating with each other. The closer the two sound speeds, the faster the pulses decay.

It is also important to emphasize that the duration of each pressure peak in the surrounding medium (Fig. 2) is  $\tau_c = 2a/c$ , where  $c$  is the speed of sound in the absorber. This has important ramifications because it affords a method for experimentally determining the bulk modulus  $B$  for particles that are small enough to present difficulties in measuring their pressures directly. The duration of a pressure peak  $\tau_c$  is for a pressure signal at a location *outside* the absorber, which makes it easier to measure using an acoustic transducer [8] than it would be close to the heated absorber. A measurement of  $\tau_c$ , along with knowledge of a particle's radius  $a$ , gives the speed of sound in the particle. When combined with the density of the particle, the bulk modulus is determined. In addition, the amplitudes of the pressures both inside and outside the absorber are proportional to  $\alpha$ , the thermal expansion coefficient of the absorber. Therefore, once  $B$  is determined by measuring  $\tau_c$ , a measurement of the amplitude of the pressure outside the absorber, where it is easier to make such measurements, allows a determination of  $\alpha$ .

To illustrate the profile of the transient for the conditions under discussion, we study the biological system of a melanosome immersed in a waterlike medium. The melanosome is a spheroidal composite of melanin found in the retinal pigment epithelial (RPE) cells of the eye [2–4]. The system is currently under intensive investigations due to its laser safety and medical applications. The melanosome is usually modeled as a highly absorbing sphere with  $\alpha_L = 1000 \text{ cm}^{-1}$ ,  $a = 1 \text{ }\mu\text{m}$ ,  $\rho_0 = 1.35 \text{ g/cm}^3$ , and  $c_v = 2.51 \text{ J/(g K)}$  while the medium can be approximated as water. We use a laser with pulse duration  $\tau_0 = 4 \times 10^{-9} \text{ s}$  and incident fluence  $I_0 = 1 \text{ J/cm}^2$ , which is known to result in damage to RPE cells [2,3]. Use of Eq. (1) gives an absorption rate of  $\dot{I}_e = 1.72 \times 10^{11} \text{ J/(g s)}$ . To fit with the conditions we are investigating at this point in the paper of  $\rho_{m0} = \rho_0$ , we approximate the density of melanosome to be that of water, and use  $\rho_0 = 1 \text{ g/cm}^3$ . Reliable numbers for the bulk modulus  $B$  and bulk thermal expansion coefficient  $\alpha$  of the melanosome have not yet been reported. In order to continue with the calculations, we use graphite as a substitute because of their chemical similarity [21], and set  $B = 39.4 \text{ GPa}$  and  $\alpha = 2.98 \times 10^{-5} \text{ K}^{-1}$ . Accurate estimates of these numbers may come from future experiments employing the present theory and results discussed in the previous paragraph.

A typical profile of pressure transients for this system is shown in Fig. 2. Pressure transients are plotted as a function of time for points inside the melanosome [Fig. 2(a):  $r = 0.6a$ ] and outside the melanosome [Fig. 2(b):  $r = 2a$ ]. From Fig. 2(b), we see that consecutive pulses have the same sign since  $c > c_m$  in this case.

To illustrate the case of  $c < c_m$ , we propose the following experiment that is easily realizable in the laboratory: an ab-

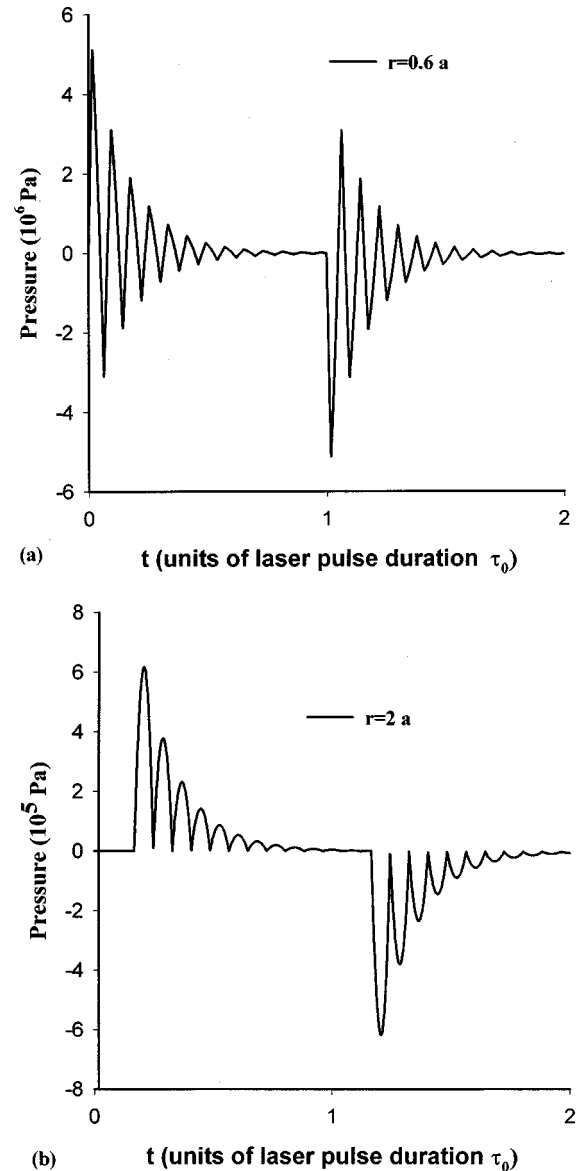


FIG. 2. Pressure generation in a melanosome surrounded by a water medium, induced by a laser of  $\tau_0 = 4 \times 10^{-9} \text{ s}$  and  $I_0 = 1 \text{ J/cm}^2$ . Typical values used for the melanosome are  $\alpha_L = 1000 \text{ cm}^{-1}$ ,  $a = 1 \text{ }\mu\text{m}$ ,  $\rho_0 = 1.35 \text{ g/cm}^3$  (approximated for this case as  $1.0 \text{ g/cm}^3$ , the value of water), and  $c_v = 2.51 \text{ J/(g K)}$ . The bulk modulus and bulk thermal expansion coefficient used for the melanosome are those of graphite:  $B = 39.4 \text{ GPa}$  and  $\alpha = 2.98 \times 10^{-5} \text{ K}^{-1}$ . Gauge pressure (in pascals) vs time (in units of  $\tau_0$ , the laser pulse duration) for a point inside the melanosome [(a)  $r = 0.6a$ ] and outside the melanosome [(b)  $r = 2a$ ]. Consecutive pulses outside the melanosome have the same sign since  $c > c_m$ .

sorbing aqueous solution of potassium chromate ( $\text{K}_2\text{CrO}_4$ ) embedded in a spherical cavity inside a transparent solid medium. A solution of 35 mg of potassium chromate per cubic centimeter yields an absorption coefficient of  $\alpha_L = 1000 \text{ cm}^{-1}$  [22]. The mechanical properties are little changed from that of water, so we use  $\rho_0 = 1 \text{ g/cm}^3$ ,  $c_v = 4.18 \text{ J/(g K)}$ ,  $B = 2.25 \text{ GPa}$ , and  $\alpha = 6.9 \times 10^{-5} \text{ K}^{-1}$ . For the solid medium, we use polystyrene, which transmits about 90% of visible light [23]. Typical values are  $B_m = 7 \text{ GPa}$  and  $\rho_{m0} \sim 1.19\text{--}1.20 \text{ g/cm}^3$  [23], which we approximate as that

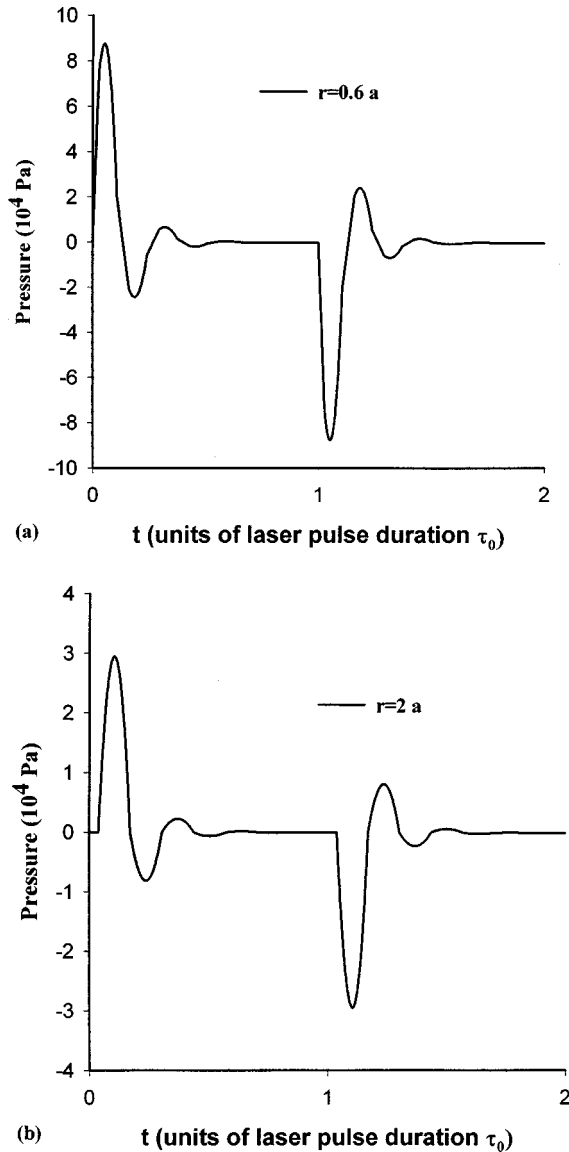


FIG. 3. Pressure generation in a potassium chromate solution surrounded by polystyrene, induced by a laser of  $\tau_0 = 10^{-6}$  s and  $I_0 = 1 \text{ J/cm}^2$ . For a solution of 35 mg of potassium chromate per cubic centimeter,  $\alpha_L = 1000 \text{ cm}^{-1}$ . For the solution we use the mechanical properties of water:  $a = 0.1 \text{ mm}$ ,  $\rho_0 = 1 \text{ g/cm}^3$ ,  $c_v = 4.18 \text{ J/(g K)}$ ,  $B = 2.25 \text{ GPa}$ , and  $\alpha = 6.9 \times 10^{-5} \text{ K}^{-1}$ . For polystyrene, we use  $B_m = 7 \text{ GPa}$  and  $\rho_{m0} \sim 1.19\text{--}1.20 \text{ g/cm}^3 \approx 1.0 \text{ g/cm}^3$ . Gauge pressure (in pascals) vs time (in units of  $\tau_0$ , the laser pulse duration) for a point inside the absorbing solution [(a)  $r = 0.6a$ ] and a point in the solid medium [(b)  $r = 2a$ ]. Consecutive pulses in the medium have opposite signs since  $c < c_m$ .

of water. We choose the size of the solution to have  $a = 0.1 \text{ mm}$ , a laser with pulse duration  $\tau_0 = 10^{-6} \text{ s}$  and fluence  $I_0 = 1 \text{ J/cm}^2$  (low enough not to evaporate the solution). In Fig. 3, we show for such an experiment the expected pressure transients plotted as a function of time for a point inside the solution [Fig. 3(a):  $r = 0.6a$ ], and outside the solution [Fig. 3(b):  $r = 2a$ ]. It is seen in Fig. 3(b) that outside the solution, the consecutive pulses have opposite signs for  $c < c_m$ . That is, the medium experiences compressive and tensile pulses alternating with each other.

### 3. $\rho_{m0} \neq \rho_0$ and $c_m \neq c$

For this most general case, the pressure transient has a complicated mathematical form given by Eqs. (24), (25), and (33). The actual profile of pressure transients however, is very similar to that in Sec. II A2 ( $\rho_{m0} = \rho_0$  and  $c_m \neq c$ ), just discussed, if the densities of the absorber and medium do not differ by much.

Again, we use the system of a melanosome immersed in a waterlike medium for demonstration. This time we use a realistic  $\rho_0 = 1.35 \text{ g/cm}^3$ , rather than approximating it to have the same value as water. In Fig. 4, we show for such a system the pressure transients plotted as a function of time for a point inside the melanosome [Fig. 4(a):  $r = 0.6a$ ] and outside the melanosome [Fig. 4(c):  $r = 2a$ ]. Except for the difference in the density, all other values for the melanosome and the laser are the same as those used in Fig. 2. Also plotted are the pressure transients calculated directly from Eqs. (4), (6), (8), (9), and (10) using the Lax algorithm of numerical solution of the partial differential equation (PDE) [24] that allows the computation of the pressure transients without going through the linearization and decoupling used to obtain the analytical results. We see from Fig. 4 that the numerical and analytical calculations agree perfectly for this system and conditions. This agreement, as well as agreement that we found for other values of the parameters, justifies our analytic approach, and shows that nonlinearities associated with the spherical geometry and the coupling of volume expansion and heating are negligible for these systems. The analytic method has the advantage of being much quicker for computations. Comparing Figs. 2 and 4, we find that the pressure transients are very similar to each other, although the pulses in Fig. 4 are no longer strictly parabolic.

### B. Ultrashort laser pulse

When the laser pulse has  $\tau_0 \ll \tau_c$ , the overlap of the pressure transients produced by the positive laser signal and negative laser signal that turns off the laser, leads to a new phenomenon. We note that for a long laser pulse, when the positive and negative pressure signals are well separated, the size of the pressure transients at a given point and the maximum pressure attained during the transients  $|\delta P|_{\text{max}}$  are inversely proportional to the laser pulse duration  $\tau_0$ . (Note that  $\dot{I}_e = I_e / \tau_0$ , where  $I_e$  is the total energy input per unit mass.) It is postulated, however, that  $|\delta P|_{\text{max}}$  will stop increasing and approach a limit when  $\tau_0$  becomes as small as some mechanical relaxation time of the system such as  $\tau_c$ . When  $\tau_0$  is below this relaxation time, the system has no time to relax and expand during the laser pulse duration, and the input energy is used with maximum efficiency in the generation of pressure. This concept, called the stress confinement condition, has often been used in estimates of the upper limit for pressure amplitudes for a given energy input [22]. In our case, this would imply that  $|\delta P|_{\text{max}}$  would become independent of  $\tau_0$  when  $\tau_0 \ll \tau_c$ .

Conditions which might exhibit stress confinement have been used in recent experiments as well as numerical work [18,19]. The experiments have shown fractured melanosome

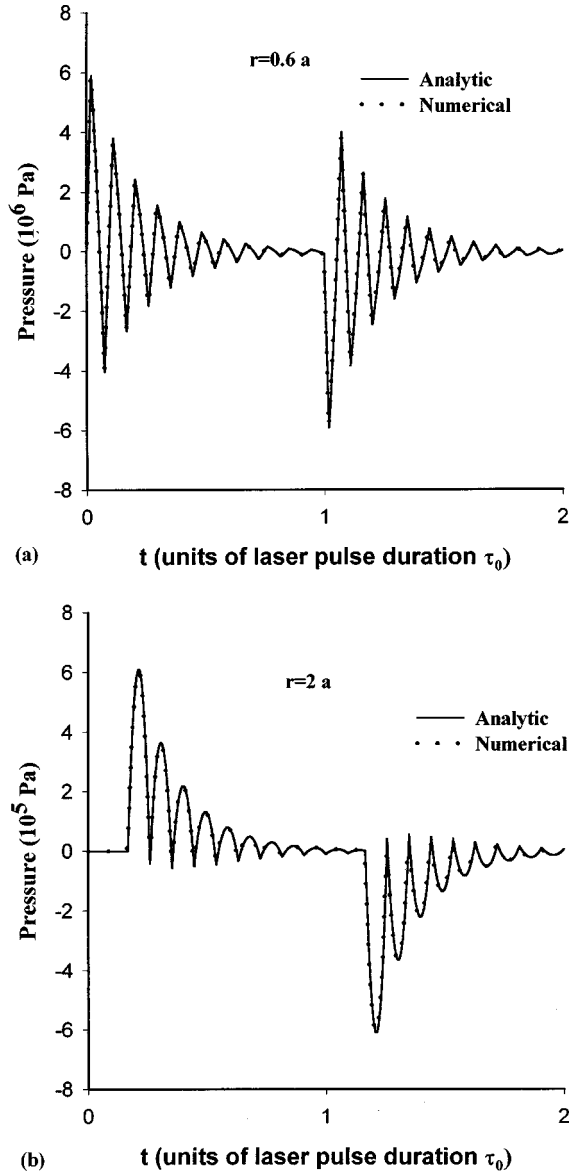


FIG. 4. Pressure generation in a melanosome surrounded by a water medium, induced by a laser of  $\tau_0 = 4 \times 10^{-9}$  s and  $I_0 = 1$  J/cm<sup>2</sup>. Values used for the melanosome are  $\alpha_L = 1000$  cm<sup>-1</sup>,  $a = 1$   $\mu$ m,  $\rho_0 = 1.35$  g/cm<sup>3</sup>, and  $c_v = 2.51$  J/(g K). The bulk modulus and bulk thermal expansion coefficient used are those of graphite:  $B = 39.4$  GPa and  $\alpha = 2.98 \times 10^{-5}$  K<sup>-1</sup>. Gauge pressure (in pascals) vs time (in units of  $\tau_0$ , the laser pulse duration) for a point inside the melanosome [(a)  $r = 0.6a$ ] and a point outside the melanosome [(b)  $r = 2a$ ]. Unlike Fig. 2, the actual value of  $\rho_0$  has been used. Also included is the results of the numerical solution which takes into account all the coupled terms in Eqs. (4), (6), (8), (9), and (10). The analytic and numerical solutions are in excellent agreement.

particles for ultrashort pulses [19]. The fractures are believed to be caused by a large tensile stress in the absorber. In a microscopic simulation of a two-dimensional absorber, Zhigilei and Garrison [20] showed tensile fracture around the core of the absorber for short laser pulses. As opposed to the idea of stress confinement, these investigations suggest that pressure amplitudes continue to increase as  $\tau_0$  is shortened, even when  $\tau_0 \ll \tau_c$ . To determine if a stress confinement regime occurs or not, a more careful study of the pressure

transients caused by ultrashort laser pulses is needed. Our analytic solution, based on macroscopic continuum mechanics, provides an opportunity for this investigation.

Our analytic solution reveals that although the maximum stress can be safely estimated by the stress confinement condition during the laser pulse, a tensile stress develops later at  $t = \tau_c/2$  that relieves the pressure. However, there is a region  $r < r_c$  inside the absorber where the  $|\delta P|_{\max}$  continues to increase as  $\tau_0$  is reduced, even when  $\tau_0 \ll \tau_c$ . In this region, the concept of stress confinement does not hold for the tensile stress. The value of  $r_c$ , which we call the critical radius, is proportional to  $\tau_0$ , and also marks a transition in the  $r$  dependence of the  $|\delta P|_{\max}$ . This phenomenon should occur in all systems with a confined absorber where the relaxing tensile pressure pulse from the outer part of the absorber converges into the geometric center. We also expect the effect to be less pronounced in lower dimensional systems, as supported by the numerical study of Paltauf and Schmidt-Kloiber [18] on a two-dimensional system.

We now demonstrate this phenomenon assuming  $\rho_{m0} = \rho_0$  and  $c_m = c$ . This case has the simplest mathematics and is sufficient to exhibit the effect of interest. First we observe from Eqs. (25) and (28) that, for long laser pulses, the  $r$  dependence of  $|\delta P|_{\max}$  changes inside the absorber, rather than at the surface: For  $r > a/2$ ,

$$|\delta P|_{\max} \left( t = \frac{r}{c} \right) = \frac{B \alpha I_e a^2}{4 r c c_v \tau_0} \sim \frac{1}{\tau_0 r}. \quad (37a)$$

For  $0 < r \leq a/2$ ,

$$|\delta P|_{\max} \left( t = \frac{a-r}{c} \right) = \frac{B \alpha I_e (a-r)}{c c_v \tau_0} \sim \frac{a-r}{\tau_0}, \quad (37b)$$

where the dependencies on  $\tau_0$  and  $r$  are explicitly displayed. Note that, for a long laser pulse,  $|\delta P|_{\max}$  is inversely proportional to  $\tau_0$ . Also, the critical radius  $r_c = a/2$  marks a transition of  $r$ -dependence from  $1/r$  to a linear dependence  $a-r$ . Physically, such a transition is necessary as we go toward smaller  $r$  to avoid infinite pressures at the origin.

For ultrashort laser pulses  $\tau_0 \ll \tau_c$ , the pressure transients at a particular point are different from those generated by longer laser pulses due to the overlap of the positive and negative signals. Let us begin with the case  $r > a$ . For a point  $r$  outside the absorber, a pressure transient reaches it at  $t = (r-a)/c$ . Before the acoustic pressure pulse is over, the transient created by the negative laser pulse that turns off the laser at  $t = \tau_0$  also arrives at  $t = \tau_0 + [(r-a)/c]$ . The effects produced by the two signals tend to cancel each other, but not completely. Detailed analysis using Eqs. (24), (25), and (28) shows that, for  $r > a$ ,

$$\delta P(r,t) = B\alpha \frac{I_e c}{4rc_v} \begin{cases} 0, & 0 < t \leq \frac{r-a}{c} \\ \frac{1}{\tau_0} \left( t - \frac{r-a}{c} \right) \left( \frac{r+a}{c} - t \right), & \frac{r-a}{c} < t \leq \tau_0 + \frac{r-a}{c} \\ \left( \tau_0 - 2t + \frac{2r}{c} \right), & \tau_0 + \frac{r-a}{c} < t \leq \frac{r+a}{c} \\ \frac{1}{\tau_0} \left( t - \tau_0 - \frac{r-a}{c} \right) \left( t - \tau_0 - \frac{r+a}{c} \right), & \frac{r+a}{c} < t \leq \tau_0 + \frac{r+a}{c} \\ 0, & \tau_0 + \frac{r+a}{c} < t. \end{cases} \quad (38)$$

Figure 5 is the profile of the pressure signal outside the focal region ( $r=2a$ ) for the same finite focusing effect in water as in Fig. 1. However, in Fig. 5 we use a laser with a much shorter pulse duration than in Fig. 1. The pulse duration in Fig. 5 is  $\tau_0 = 10^{-9}$  s, which is much shorter than the system's mechanical relaxation time of  $\tau_c = 4 \times 10^{-8}$  s. Under these conditions of  $\tau_0 \ll \tau_c$ , the negative tensile pressure pulse of Fig. 1(b) occurs before the positive compressive pulse has finished, and Fig. 5 can be viewed as the overlap of the positive and negative pulses. The negative tensile wave travels out from the surface starting at  $\tau_0$  when the laser is turned off. Due to their width, the time between the compressive maximum of the peak and the tensile minimum of the

trough is equal to  $\tau_c - \tau_0 \approx \tau_c$ . This is especially important in considering material damage or failure, since the forces that are created depend on the rate of change of the pressure. Equally important is the result that the rise time to the compressive peak, and the decay time from the tensile trough, are now on the order of  $\tau_0$ . Therefore, as the laser pulse duration is shortened, greater forces occur, and material failure in the medium becomes more likely.

We see from Eq. (38) that the maximum pressures occur at  $t = \tau_0 + [(r-a)/c]$  and  $t = (r+a)/c$  (corresponding, respectively, to compressive and tensile). For the ultrashort  $\tau_0$  limit,

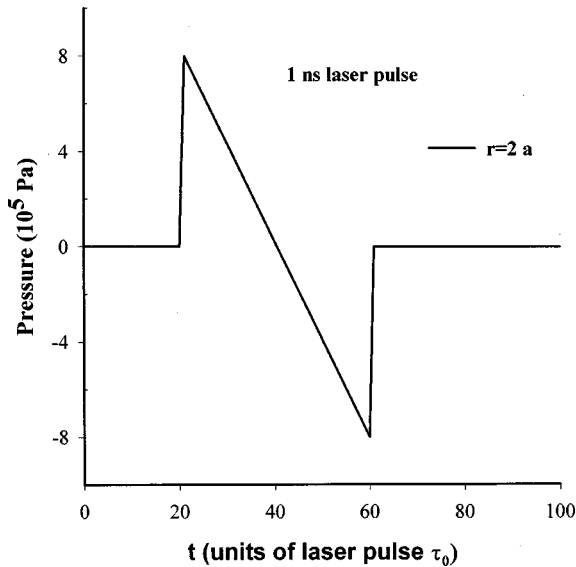


FIG. 5. Finite focusing effect in water for ultrashort laser pulses. Gauge pressure (in pascals) vs time (in units of  $\tau_0$ , the laser pulse duration) for a point outside the focus  $r=2a$ . Values used for water are  $\rho_0 = 1$  g/cm<sup>3</sup>,  $c_v = 4.18$  J/(g K),  $B = 2.25$  GPa, and  $\alpha = 6.9 \times 10^{-5}$  K<sup>-1</sup>. The laser pulse, with a focal size of  $a = 30$   $\mu$ m, carries the same fixed energy of  $10^{-5}$  J as in Fig. 1. Under these conditions of  $\tau_0 \ll \tau_c$ , the negative tensile pressure pulse occurs before the positive compressive pulse has finished, and the resulting transient can be viewed as the overlap of the positive and negative pulses. The time between the compressive peak and the tensile trough is approximately equal to  $\tau_c = 2a/c$ .

$$|\delta P|_{\max} = B\alpha \frac{I_e c}{4rc_v} \left( \frac{2a}{c} - \tau_0 \right) \sim \frac{1}{r}. \quad (39)$$

We see from Eq. (39) that  $|\delta P|_{\max}$  indeed approaches a limit when  $\tau_0$  decreases. For  $r > a$ , the stress confinement limit is valid and the  $r$  dependence of  $|\delta P|_{\max}$  is  $1/r$ .

For  $r \leq a$  and deep in the sphere, the pressure at a point  $r$  first increases linearly with time due to the uniform heating. The pressure stops building up when the laser is turned off, and remains at a constant value. Meanwhile, the tensile wave associated with the positive laser signal due to the expansion at the surface is moving inward from the surface and arrives at  $t = (a-r)/c$ . When this tensile wave reaches the point  $r$ , it starts to reduce the pressure at a large rate which increases as  $1/\tau_0$ . It then takes  $2r/c$  for this wave to travel to the origin and reflect back as a compressive wave. During this time, the tensile stress can reach large negative values that can fracture the absorber. The shorter the laser pulse, the greater the tensile stress attained. Once the compressive reflection arrives, the tensile stress continues to increase but at a much slower rate.

On the other hand, for larger values of  $r$  inside the melanosome, where the rate of increasing tensile stress is not as large, the tensile stress may not have time to build up to a large value. This is because starting at  $\tau_0$  when the laser is turned off, equivalent to a negative laser fluence, a compressive wave set off by the negative laser signal starts to travel in from the surface. The compressive wave from the surface will arrive at  $r$  at  $t = \tau_0 + [(a-r)/c]$ . If this compressive

wave arrives before the compressive reflection from the origin returns to  $r$  at  $t=(a+r)/c$ , the tensile stress does not have enough time to build up to a large value. We define the critical radius  $r_c$  as the radius where the compressive wave, traveling in from the surface that is associated with the negative laser signal, arrives at the same instant that the compressive wave from the positive laser signal returns back after reflection at the origin.  $r_c$  separates region I ( $r \leq r_c$ ), where the first transient from the positive laser returns back first, and region II ( $r > r_c$ ), where the compressive wave traveling in from the surface that is associated with the negative laser

signal, arrives first.  $r_c$  occurs for a value of  $r$  such that  $(a+r)/c$  is equal to  $\tau_0 + [(a-r)/c]$ , and gives

$$r_c = \frac{c\tau_0}{2}. \quad (40)$$

We will show that  $r_c$  also marks the transition for the  $r$  dependence of  $|\delta P|_{\max}$ . Furthermore, for  $r \leq r_c$ ,  $|\delta P|_{\max}$  is proportional to  $1/\tau_0$  even for ultrashort pulses, but in region II we show that  $|\delta P|_{\max}$  is only weakly dependent on  $\tau_0$ . Using Eqs. (24), (25), and (28), for  $r \leq a$  we have the following. Region I ( $r \leq r_c$ ),

$$\delta P(r,t) = B\alpha \frac{I_e}{c_v} \begin{cases} \frac{t}{\tau_0}, & 0 < t \leq \tau_0 \\ 1, & \tau_0 < t \leq \frac{a-r}{c} \\ 1 - \frac{c}{4r\tau_0} \left( t - \frac{a-r}{c} \right) \left( t + \frac{a+r}{c} \right), & \frac{a-r}{c} < t \leq \frac{a+r}{c} \\ 1 - \frac{t}{\tau_0}, & \frac{a+r}{c} < t \leq \tau_0 + \frac{a-r}{c} \\ \frac{c}{4r\tau_0} \left( t - \tau_0 - \frac{a-r}{c} \right) \left( t - \tau_0 + \frac{a+r}{c} \right) - \frac{t}{\tau_0} + 1, & \tau_0 + \frac{a-r}{c} < t \leq \tau_0 + \frac{a+r}{c} \\ 0, & \tau_0 + \frac{a+r}{c} < t. \end{cases} \quad (41a)$$

Region II ( $r > r_c$ ),

$$\delta P(r,t) = B\alpha \frac{I_e}{c_v} \begin{cases} \frac{t}{\tau_0}, & 0 < t \leq \tau_0 \\ 1, & \tau_0 < t \leq \frac{a-r}{c} \\ 1 - \frac{c}{4r\tau_0} \left( t - \frac{a-r}{c} \right) \left( t + \frac{a+r}{c} \right), & \frac{a-r}{c} < t \leq \tau_0 + \frac{a-r}{c} \\ 1 - \frac{c}{4r} \left( 2t - \tau_0 + \frac{2r}{c} \right), & \tau_0 + \frac{a-r}{c} < t \leq \frac{a+r}{c} \\ \frac{c}{4r\tau_0} \left( t - \tau_0 - \frac{a-r}{c} \right) \left( t - \tau_0 + \frac{a+r}{c} \right) - \frac{t}{\tau_0} + 1, & \frac{a+r}{c} < t \leq \tau_0 + \frac{a+r}{c} \\ 0, & \tau_0 + \frac{a+r}{c} < t. \end{cases} \quad (41b)$$

Detailed analysis shows that, in region I, the maximum tensile stress occurs at  $t = \tau_0 + [(a-r)/c]$ . For the ultrashort  $\tau_0 \ll \tau_c$  limit [as well as the limit of small  $r$  since  $r \leq r_c \sim \tau_0$  from Eq. (40)], we have

$$|\delta P|_{\max} = B \alpha (a-r) \frac{I_e}{c c_v \tau_0} \sim \frac{1}{\tau_0}. \quad (42a)$$

In region II, a maximum tensile stress occurs at  $t = [(a+r)/c]$ . In the ultrashort  $\tau_0$  limit, we have

$$|\delta P|_{\max} = B \alpha \frac{I_e c}{4 r c_v} \left( \frac{2a}{c} - \tau_0 \right) \sim \frac{1}{r}. \quad (42b)$$

From Eq. (42), we see that, while in region II  $|\delta P|_{\max}$  becomes independent of  $\tau_0$  as  $\tau_0$  goes toward zero, in region I  $|\delta P|_{\max}$  continues to increase as we reduce  $\tau_0$ . The  $r$  dependence of  $|\delta P|_{\max}$  in region I is linear, and becomes independent of  $r$  at ultrashort laser pulses as  $r_c$  approaches zero, as opposed to the  $1/r$  dependence in region II.  $r_c$ , being proportional to  $\tau_0$ , decreases as  $\tau_0$  decreases. This allows the boundary of region II to move inward toward smaller  $r$ . These inner locations of region II ( $r > r_c$  but small  $r$ ) continue to experience high  $|\delta P|_{\max}$  when they switch from being in region I to region II, because the tensile stress in region II depends on  $1/r$ . However, the tensile stress in region I continues to be a little higher, with the maximum at the origin being  $a/(a-r_c)$  larger than at  $r_c$ . The picture presented by this model in which the tensile stress at the center continues to increase as  $\tau_0$  decreases is quite different from the idea of a stress confinement limit, and should serve as a new approach for calculating the acoustic damage in real biological systems.

To illustrate the effect, we use the example of the finite focusing effect in water shown in Fig. 1. Again we use a focal size of  $a = 30 \mu\text{m}$  and  $\tau_c = 2a/c = 4 \times 10^{-8}$  s. The laser pulse carries the same fixed energy of  $10^{-5}$  J as in Fig. 1. However, we use a series of much shorter pulses in a decreasing order:  $\tau_0 = 10^{-8}$ ,  $5 \times 10^{-9}$ ,  $2 \times 10^{-9}$ , and  $10^{-9}$  s. The first laser pulse  $\tau_0 = 10^{-8}$  s has a  $r_c = (\tau_0/\tau_c)a = 0.25a$  while the last one has a  $r_c = 0.025a$ . We choose two points inside the absorber:  $r = 0.01a$ , which is in region I for every laser pulse; and  $r = 0.3a$ , which is in region II for every laser pulse. The pressures as a function of time for these two  $r$ 's are shown in Fig. 6. For comparison, we use the same real unit of time for all laser pulses.

From Fig. 6, we see that in region I the tensile stress keeps increasing with decreasing laser pulse duration, while in region II the maximum of the stress amplitude changes very little from  $\tau_0 = 10^{-8}$ – $10^{-9}$  s. Notice that at  $\tau_0 = 10^{-8}$  s, the amplitudes at  $r = 0.01a$  and  $0.3a$  are of the same order, but at  $\tau_0 = 10^{-9}$  s, they differ by an order of magnitude.

This phenomenon is quite general. In Fig. 7, we show results for the general conditions where  $\rho_{m0} \neq \rho_0$  and  $c_m$

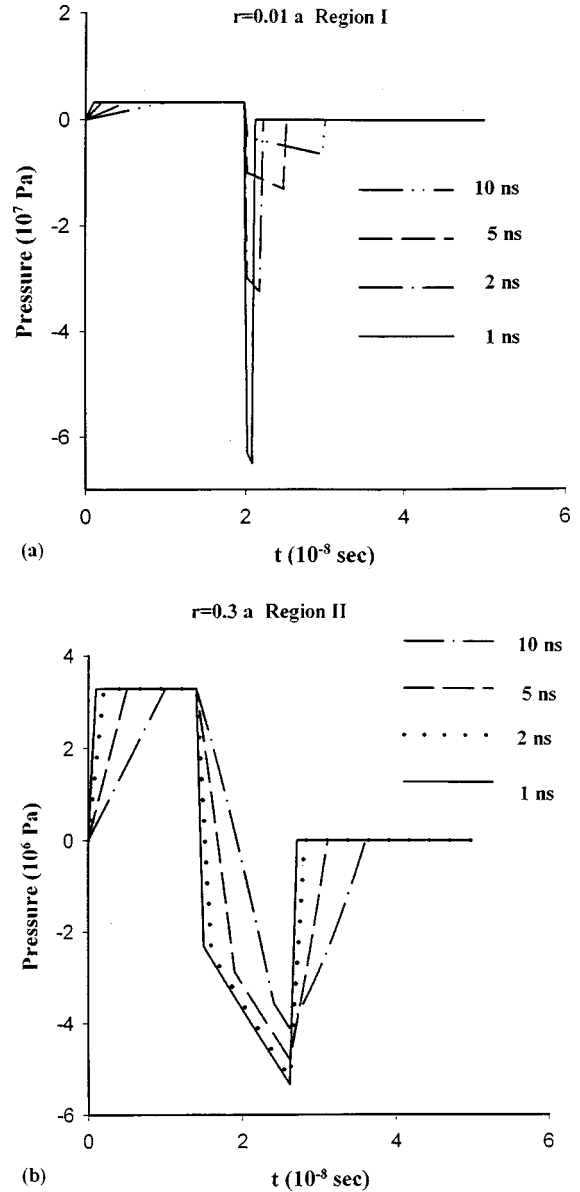


FIG. 6. Finite focusing effect in water for ultrashort laser pulses. In decreasing order of pulse duration  $\tau_0 = 10^{-8}$ ,  $5 \times 10^{-9}$ ,  $2 \times 10^{-9}$ , and  $10^{-9}$  s. The gauge pressure (in pascals) vs time (in seconds) for a point in region I ( $r \leq r_c$ ) at  $r = 0.01a$ , and for a point in region II ( $r > r_c$ ) at  $r = 0.3a$ . Values used for water are  $\rho_0 = 1 \text{ g/cm}^3$ ,  $c_v = 4.18 \text{ J/(g K)}$ ,  $B = 2.25 \text{ GPa}$ , and  $\alpha = 6.9 \times 10^{-5} \text{ K}^{-1}$ . The laser pulse, with a focal size of  $a = 30 \mu\text{m}$ , carries the same fixed energy of  $10^{-5}$  J as in Fig. 1. In region I, the tensile stress continues to increase with decreasing laser pulse duration, while in region II the stress amplitude changes very little from  $\tau_0 = 10^{-8}$  to  $10^{-9}$  s.

$\neq c$ . This is the same laser-melanosome system described in Fig. 4, which has a  $\tau_c = 2a/c = 3.7 \times 10^{-10}$  s. We choose a laser with  $\tau_0 = 10^{-11}$  s, which gives  $r_c = 0.027a$ . We choose an observation point at  $r = 0.01a$  which is inside region I. Figure 7 shows that under these general conditions, a series of tensile spikes appears with an interval of  $\tau_c$  between spikes. The appearance of a series of tensile spikes is in contrast with the special case of  $\rho_{m0} = \rho_0$  and  $c_m = c$ , where

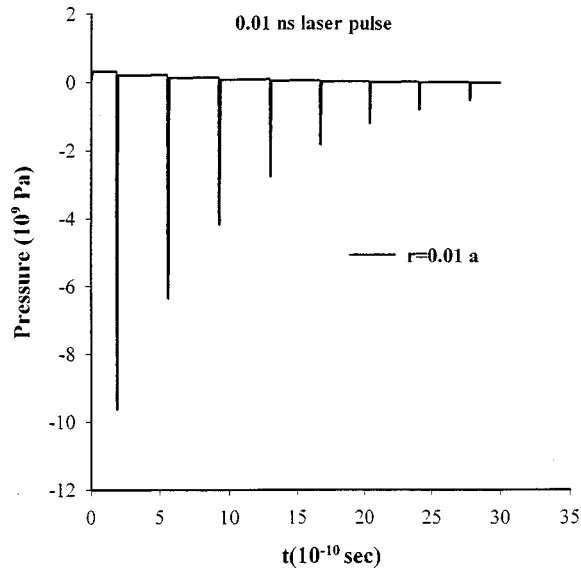


FIG. 7. Pressure generation in a melanosome surrounded by a water medium, induced by an ultrashort laser of  $\tau_0 = \times 10^{-11}$  s and  $I_0 = 1 \text{ J/cm}^2$ . Values used for the melanosome are  $\alpha_L = 1000 \text{ cm}^{-1}$ ,  $a = 1 \text{ }\mu\text{m}$ ,  $\rho_0 = 1.35 \text{ g/cm}^3$ , and  $c_v = 2.51 \text{ J/(g K)}$ . The bulk modulus and bulk thermal expansion coefficient used are those of graphite:  $B = 39.4 \text{ GPa}$  and  $\alpha = 2.98 \times 10^{-5} \text{ K}^{-1}$ . Gauge pressure (in pascals) vs time (in seconds) for a point inside region I ( $r = 0.01a$  and  $r_c = 0.027a$ ). A series of tensile spikes is observed in this case.

only a single tensile spike is observed.

Finally, we mention that in the limit of  $\tau_0 = 0$ , the tensile stress appears to approach infinity, which is unphysical. Eventually, as the laser pulse duration is shortened, nonlinearities will play a role. The critical radius  $r_c$ , which is proportional to  $\tau_0$  in Eq. (40), also has a lower bound, which we presume to be the microscopic spacing. Continuum mechanics, upon which the present treatment is based, fails when the important scale is comparable to atomic or molecular spacings. It is then necessary to ask about the fate of the large tensile stress when  $r_c$  approaches atomic spacings,

where short wavelength response is important. A microscopic investigation may reveal more interesting features at this limit.

#### IV. CONCLUSION

We have investigated the pressures expected to result when a laser pulse is incident on a spherical absorber using both numerical and analytical techniques. We have looked at laser pulses of duration both greater and shorter than the mechanical relaxation time of the absorber. The pressure profiles result from a uniform compressive pressure increase throughout the absorber while the laser is on, along with a tensile wave traveling in from the surface due to the expansion of the absorber. When the pulse is turned off the uniform compressive buildup stops, but a compressive wave traveling in from the surface commences.

In addition, reflections from the origin of first the tensile wave, and then the compressive wave occur, sending waves of the opposite sign outward. These reflections superimpose their effects. When the mechanical impedance of the surrounding medium is not matched to the absorber, the outward moving waves are partially reflected back into the absorber, and partially transmitted.

The net effect of these different pressure transients depends on their order of occurrence which is determined by the length of the laser pulse, and point of observation. Of especial interest, we find that deep inside the absorber,  $r < r_c$ , there is a region where the concept of stress confinement does not hold. Even when the laser pulse duration is much shorter than the mechanical relaxation time of the absorber,  $\tau_0 \ll \tau_c$ , as  $\tau_0$  is shortened the magnitude of the tensile stress continues to increase. The large tensile stresses that develop at the center of the absorber may be of critical importance in damaging or fracturing the absorber.

#### ACKNOWLEDGMENT

The authors wish to thank the U.S. Air Force Office of Scientific Research for funding this work through Grant No. F49620-96-1-0438.

- 
- [1] O. Yavas, P. Leiderer, H. K. Park, C. P. Grigoropoulos, C. C. Poon, W. L. Leung, N. Do, and A. C. Tam, *Phys. Rev. Lett.* **70**, 1830 (1993).
- [2] B. S. Gerstman, C. R. Thompson, S. L. Jacques, and M. E. Rogers, *Lasers Surg. Med.* **18**, 10 (1996).
- [3] C. R. Thompson, B. S. Gerstman, S. L. Jacques, and M. E. Rogers, *Bull. Math. Biol.* **58**, 513 (1996).
- [4] R. Birngruber, V. P. Gabel, and F. Hillenkamp, *Health Phys.* **44**, 519 (1983).
- [5] R. G. Brewer and K. E. Riechhoff, *Phys. Rev. Lett.* **13**, 334 (1964).
- [6] H. Chiao, C. Townes, and N. Stoichef, *Phys. Rev. Lett.* **12**, 592 (1964).
- [7] R. P. Hawkes, T. J. Farrell, M. S. Patterson, and R. A. Weersink, *Proc. SPIE* **2975**, 208 (1997).
- [8] A. Vogel, S. Busch, and U. Parlitz, *J. Acoust. Soc. Am.* **100**, 148 (1996).
- [9] V. I. Danilvoskaya, *Prikl. Mat. Mekh.* **14**, 316 (1950); **16**, 341 (1952).
- [10] E. Sternberg and J. G. Chakravorty, *J. Appl. Mech.* **37**, 503 (1959).
- [11] R. M. White, *J. Appl. Phys.* **34**, 3559 (1963).
- [12] R. Bullough and J. J. Gilman, *J. Appl. Phys.* **37**, 2283 (1966).
- [13] L. S. Gournay, *J. Acoust. Soc. Am.* **40**, 1322 (1966).
- [14] C. L. Hu, *J. Acoust. Soc. Am.* **46**, 728 (1969).
- [15] A. A. Oraevsky, S. L. Jacques, and F. K. Tittel, *J. Appl. Phys.* **78**, 1281 (1995).
- [16] R. Courant and K. Friedrichs, *Supersonic Flow and Shock*

- Waves* (Springer-Verlag, New York, 1948).
- [17] M. Frenz, G. Paltauf, and H. Schmidt-Kloiber, *Phys. Rev. Lett.* **76**, 3546 (1996).
- [18] G. Paltauf, H. Schmidt-Kloiber, *Proc. SPIE* **3254**, 112 (1998).
- [19] C. P. Lin, presentation at Photonics West, 1998 San Jose, CA (unpublished).
- [20] L. V. Zhigilei and B. J. Garrison, *Appl. Surf. Sci.* **127-129**, 142 (1998); *Proc. SPIE* **3254**, 135 (1998).
- [21] W. N. Reynolds, *Physical Properties of Graphite* (Elsevier, Amsterdam, 1968).
- [22] A. A. Oraevsky, S. L. Jacques, and F. K. Tittel, *Appl. Opt.* **36**, 402 (1997).
- [23] I. I. Rubin, *Handbook of Plastic Materials and Technology* (Wiley, New York, 1990).
- [24] W. H. Press, *Numerical Recipes* (Cambridge University Press, Cambridge, 1986).